

Chapter 9

Cortical Phase Transitions as an Effect of Topology of Neural Network

Ilenia Apicella, Silvia Scarpetta and Antonio de Candia

Abstract Understanding the emerging of cortical dynamical state, its functional role, and its relationship with network topology, is one of the most interesting open questions in computational neuroscience. Spontaneous cortical dynamics often shows spontaneous fluctuations with UP/DOWN alternations and critical avalanches which resemble the critical fluctuations of a system posed near a non-equilibrium noise-induced phase transition. A model with structured connectivity and dynamical attractors has been shown to sustain two different dynamic states and a phase transition with critical behaviour is observed. We investigate here which are the features of the connectivity which permit the emergence of the phase transition and the large fluctuations near the critical line. We start from the original connectivity, that comes from the learning of the spatiotemporal patterns, and we shuffle the presynaptic units, leaving unchanged both the postsynaptic units and the value of the connections. The original structured network has a large clustering coefficient, since it has more directed connections which cooperate to activate a precise order of neurons, respect to randomized network. When we shuffle the connections we reduce the clustering coefficient and we destroy the spatiotemporal pattern attractors. We observe that the phase transition is gradually destroyed when we increase the ratio of shuffled connections, and already at a shuffling ratio of 70% both the phase transition and its critical features disappear.

I. Apicella · S. Scarpetta (✉)
Department of Physics “E.R. Caianiello”, University of Salerno, Fisciano, SA, Italy
e-mail: sscarpetta@unisa.it

S. Scarpetta
INFN Salerno Group, Fisciano, SA, Italy

A. de Candia
Department of Physics, University of Naples “Federico II”, Naples, Italy

A. de Candia
INFN Naples Branch, Complesso Universitario Monte S. Angelo, Naples, Italy

A. de Candia
CNR-SPIN, Naples Branch, Naples, Italy

9.1 Introduction

Thanks to recent experimental techniques, which allow to record the activity of many neurons simultaneously (both in-vivo and in-vitro), it is easier studying the complex collective dynamics emerging in highly connected networks of neurons, such as cortical networks. Spontaneous cortical activity can show critical collective features, such as the alternation between DOWN states of network quiescence and UP states of neural depolarization, observed in different system and conditions (both in-vitro [1–3] and in-vivo during slow-wave sleep, anesthesia and quiet walking [4, 5]).

Many recent works confirm the idea that brain operates close to a critical point (or close to a spinodal point), at which information processing is optimized [6–8], so that it is interesting to investigate the role of criticality on cognitive activities or brain diseases and so on.

In this paper we focus on the presence of phase transition between UP and DOWN states; it should be important to emphasize that the power laws of avalanches size and duration distributions in our model has been shown to agree with experimental data of critical exponents of size and time avalanches distributions [9].

Many experiments both in-vitro [10, 11] and in-vivo [12–15] have demonstrated that cortical spontaneous activity occurs in precise spatio-temporal patterns. In this paper we study the spontaneous cortical dynamics of a neural network, in which a phase transition between replay and not-replay of stored spatiotemporal patterns emerges.

We call “UP state” the regime in which we have high firing rate with the replay of one of stored patterns, index of high correlated activity. Instead the “DOWN state” is the regime of quiescence without replay of pattern. Between this two states, a critical regime exists, with the alternation of UP and DOWN states. In this regime there is an intermitted replay of spatiotemporal pattern.

Noise level and strength of connections are the control parameters we change during the investigation, then we calculate firing rate and normalized variance, defined in next section.

As we shall see later an high firing rate doesn’t necessarily imply an UP state, because if we change the topology of network we don’t always observe retrieval pattern when firing rate is high and we can have uncorrelated Poissonian activity even at high rates. This change of topology consists of shuffling the connections thanks to a shuffling procedure discussing below. This procedure allows us to study the spontaneous dynamics of network with different position of connections, keeping unchanged their values, getting very different and interesting regimes of activity.

9.2 The Model

In order to simulate the spontaneous activity of a slice of brain cortex, we have a network of N spiking neurons, modeled as LIF (Leaky Integrate-and-Fire) units and represented by SRM (Spike Response Model) of Gerstner [16], in presence of a

Poissonian noise distribution. Neurons are connected by a sparse connectivity with the possibility to shuffle a fraction of the connections, in order to understand the role of topology in spontaneous cortical dynamics.

If we label with index i the postsynaptic neuron and with the index j the presynaptic one, when the neuron i does not fire, the postsynaptic membrane potential is:

$$u_i(t) = \sum_j \sum_{t_j < t_j < t} J_{ij} (e^{-(t-t_j)/\tau_m} - e^{-(t-t_j)/\tau_s}) + \sum_{\hat{t}_i < \hat{t}_i < t} J_i (e^{-(t-\hat{t}_i)/\tau_m} - e^{-(t-\hat{t}_i)/\tau_s}) \quad (9.1)$$

The Eq. (9.1) has two contributions: the first one is related to the connections strength, because J_{ij} is the connection strength between pre- and postsynaptic neurons; the second contribution is related to the noise of network, because \hat{J}_i is extracted from a Gaussian distribution with mean 0 and standard deviation $\sigma = \sqrt{\alpha/\rho \sum_j J_{ij}^2}$, where α is the “noise level” of the network and $\rho = 1 \text{ ms}^{-1}$ is the rate of Poissonian distribution $P(t) \propto e^{-\rho t}$. In the Eq. (9.1) τ_m is the characteristic time of membrane (in this paper $\tau_m = 10 \text{ ms}$), τ_s is the characteristic time of synapse (in this paper $\tau_s = 5 \text{ ms}$), t_j are the spike times of neuron j , \hat{t}_i are the times of noise events releasing a random charge at some point of membrane of neuron i .

The (9.1) is the solution of a differential equation, describing a RC circuit, because in LIF model each unit has a membrane capacity C and a resistance R in parallel, so that we have for neuron i :

$$\frac{du_i(t)}{dt} = -\frac{u_i(t)}{\tau_m} + \frac{I_i(t)}{C} \quad (9.2)$$

with $\tau_m = RC$ and $I_i(t)$ is the input current, given by $I_i(t) = \sum_j \sum_{t_j < t_j < t} \frac{Q_{ij}}{\tau_s} e^{-(t-t_j)/\tau_s} + \sum_{\hat{t}_i < \hat{t}_i < t} \frac{\hat{Q}_i}{\tau_s} e^{-(t-\hat{t}_i)/\tau_s}$, where Q_{ij} is the total charge released at the synapse between neuron i and j and \hat{Q}_i is a random charge released at some point of the membrane of neuron i . Q_{ij} and \hat{Q}_i are related to J_{ij} and \hat{J}_i respectively by the relations: $J_{ij} = \frac{Q_{ij}}{C(1-\frac{\tau_s}{\tau_m})}$ and $\hat{J}_i = \frac{\hat{Q}_i}{C(1-\frac{\tau_s}{\tau_m})}$. When the membrane potential $u_i(t)$ reaches the threshold θ , the unit emits a spike and then $u_i(t)$ is reset to zero, its resting value.

So far we have described the single unit. Since we want to investigate the effects of topology on network dynamics we build a structured connectivity that gives rise to a complex dynamics with a rich phases space, and then we shuffle the connections to check if crucial changes happen also in the dynamics. In the next section we will talk about the process of creation of the network connectivity, thanks to the “learning” and “pruning” procedures, and then we will describe the shuffling procedure.

9.2.1 Learning and Pruning Procedures

We set synapse strengths J_{ij} at the beginning with the “learning” procedure, inspired by STDP (Spike Timing Dependent Plasticity). Then, during the simulation we hold fixed J_{ij} , i.e. we don’t use short term plasticity for sake of simplicity. Note that the sign of J_{ij} represent the type of synapse: if $J_{ij} < 0$ the synapse is inhibitory, while if $J_{ij} > 0$ it is excitatory. With this procedure we store $\mu = 1, 2, \dots, P$ phase-coded patterns in the network connections, i.e. periodic ordered trains of spikes t_i^μ with period T^μ and with one spike per neuron and per cycle. Because of such periodic spikes train, the strength of connection J_{ij} changes:

$$\delta J_{ij} = H_i \sum_{n=-\infty}^{\infty} A(t_i^\mu - t_j^\mu + nT^\mu) \quad (9.3)$$

where $A(\tau)$ is a function of time, called “learning window”, inspired to STDP, with $\tau = t_i^\mu - t_j^\mu + nT^\mu$. t_i^μ and t_j^μ are pre- and postsynaptic spikes time in pattern μ respectively, H_i is a constant that sets the strength of the connections, depending on the postsynaptic neuron. This learning procedure assures the balance between excitation and inhibition, i.e. $\sum_i J_{ij} = 0$.

To take into account the heterogeneity of neurons, we use two values of H_i : H_0 for “normal” neurons and $H_i = 3H_0$ for “leader” neurons, i.e. neurons that with higher incoming connection strengths amplify activity initiated by noise. In other words, leaders are neurons the ones which fire more than others, and they give rise to a cue able to initiate the short collective replay. They are chosen as a fraction of 3% of neurons with consecutive phases, for each pattern μ .

To improve the model’s biological plausibility, we delete some connections to make the connectivity sparse. With the “pruning” procedure we cut a fraction f_{prune}^+ (70%) of positive (excitatory) connections with the lowest value and a fraction $f_{prune}^{-,i}$ (depending on postsynaptic neuron) of negative (inhibitory) connections with the lowest absolute value. As it happens before pruning, also after pruning still there is a balance of positive and negative connections offering each postsynaptic unit, i.e. $\sum_i J_{ij} = 0$. In this way, only a part of connections survives: 27% of $N(N-1)$ connections are negative, 12% of $N(N-1)$ connections are positive, the other ones are equal to zero. In such a way we get a structured and sparse connectivity.

9.2.2 Shuffling Procedure

We investigate the effects of shuffling procedure on network dynamics. We start from the structured and sparse connectivity coming from learning and pruning procedures, and we apply a shuffling procedure. In such a way the network topology changes, but the strength of connections is preserved. Let’s consider the connection J_{ij} , picked up randomly. Given the postsynaptic neuron i , we change the presynaptic neuron

j with another one k , chosen randomly among other neurons of the network. We use the strength of J_{ij} for the new connection J_{ik} , i.e. $J_{ik} = J_{ij}$ and then we put the old connection J_{ij} to zero. We repeat this procedure for a fraction of connections or all the connections of the network. Not only the strength of connections remains the same, but also the balance between inhibitory and excitatory connections entering each unit is preserved. In this way we have the possibility to investigate the spontaneous dynamics of the same model but with different network topology, from a structured connectivity to a random connectivity, with the same value of connections.

The key parameters are: the noise level α , the strength of connection H_0 , expressed in units of the threshold θ of the neurons, and the fraction of connections we change cs , that is the ratio between the number of times we make the shuffling procedure and the number of connections, so we can have different situations from $cs = 0$ (structured connectivity) to $cs = 1$ (when all the connections are shuffled). For each cs we want to investigate, we change the value of α and H_0 , and we calculate the spiking rate and the normalized variance. The normalized variance is defined as $\hat{\sigma} = \frac{\sigma}{\langle r \rangle}$, where $r = \frac{n_{tot}}{N\Delta}$ is the rate, with n_{tot} total number of spikes in the time interval Δ , and $\sigma = N\Delta \langle r^2 \rangle - N\Delta \langle r \rangle^2$ is the variance. Explaining r , the normalized variance can be written as $\hat{\sigma} = \frac{\langle n_{tot}^2 \rangle - \langle n_{tot} \rangle^2}{\langle n_{tot} \rangle}$. Note that if neurons are uncorrelated and Poissonian then $\langle n_{tot}^2 \rangle - \langle n_{tot} \rangle^2 = \langle n_{tot} \rangle$. As a consequence the normalized variance is equal to 1. Therefore if normalized variance is different from 1, this means that or (1) neurons are not uncorrelated or (2) each unit is not Poissonian. To understand the importance of topology in this dynamics we calculate the clustering coefficient of the network. The clustering coefficient (C) of a node of the network is a measure of the number of edges that exist between its nearest neighbors [17]. It is defined as

$$\bar{C} = \frac{\sum_{i=1}^N \left[\sum_{j,k \in \Delta(i)} \Gamma(j \rightarrow k) \right]}{\sum_{i=1}^N z_i(z_i - 1)} \quad (9.4)$$

where $\Delta(i)$ is the set of nodes j such that there is a connection from i to j , z_i is the number of nodes in $\Delta(i)$, and $\Gamma(j \rightarrow k)$ is one if there is a connection from j to k , zero otherwise.

Structured network has more clusters of directed connections which cooperate to activate a precise order of neurons, respect with randomized network. A dense local clustering coefficient we observe in the structured network (cs close or equal to 0) remembers the regular topology of a network, while the clustering coefficient is close to 0, from a particular value of cs close to 0.7 up to $cs = 1$ (random network). We calculate the normalized clustering coefficient, defined as $C = \frac{\bar{C} - C_1}{C_0 - C_1}$, where C_0 is clustering for zero shuffling, and C_1 is for randomized network and \bar{C} is the clustering coefficient of other intermediate cases of networks.

So we have $C = 1$ for $cs = 0$, i.e. a network with structured connectivity and $C = 0$ for $cs = 1$, i.e. a random connectivity (Fig. 9.1a). In the next section we will show the main results we have got, focusing our attention in particular on three dif-

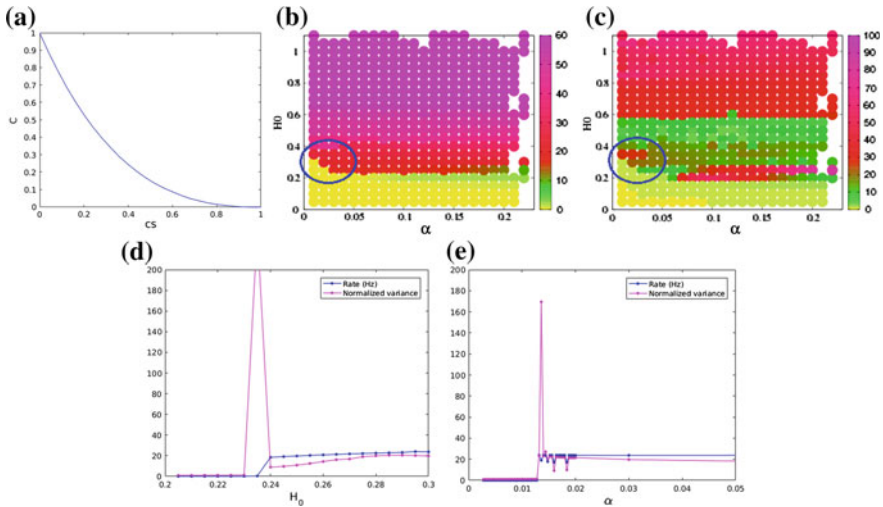


Fig. 9.1 **a** Changes of Topology. Normalized clustering coefficient $C = (\bar{C} - C_0)/(C_1 - C_0)$, where C_0 is clustering for zero shuffling, and C_1 is for randomized network, as a function of shuffled connections cs . From a value of cs close to 0.7 the clustering coefficient approaches to 0, as happens for a random network. A non-equilibrium phase transition occurs in the spontaneous dynamics of a network of $N = 3000$ neurons with structured connectivity ($cs = 0$). The rate (**b**) and the normalized variance (**c**) are shown as a function of noise intensity α and synaptic strength factor H_0 . One can see a sharp transition from a region of Poissonian quiescence, with low rate and normalized variance close to 1 (yellow points in figure **b** and **c**) to a region of correlated high rate activity (red points in figure **b** and magenta points in figure **c**), with high values of both rate and normalized variance. Between them there is an intermediate region in which the rate gradually grows and the normalized variance has a peak, index of a transition (in blue circle). **d** Rate and normalized variance are shown as a function of H_0 for fixed $\alpha = 0.03 \text{ ms}^{-1}$. Note that the transition between quiescence state and high correlated activity occurs when the rate grows and the normalized variance has a peak, for a particular value of connection strength, corresponding to the region in blue circle of figure **b** and **c**. **e** Rate and normalized variance are shown as function of α for fixed value of $H_0 = 0.3$. Note that also in this direction there is an abrupt growing of rate and a peak of normalized variance

ferent cases of topology: $cs = 0$ (structured connectivity coming from the learning), $cs = 1$ (random connectivity, when all the connections are shuffled) and $cs = 0.63$ (an intermediate case, when only 63% of connections are shuffled). We will observe three completely different behaviors.

9.3 Results

In order to study the spontaneous dynamics, we calculate the firing rate (number of spike per neuron and time interval) and the normalized variance (defined above) changing the value of noise level α and strength of connections H_0 . For a network with structured connectivity ($cs = 0$) results are shown in Fig. 9.1. In this case we observe a transition from a regime of quiescence characterized by both low values

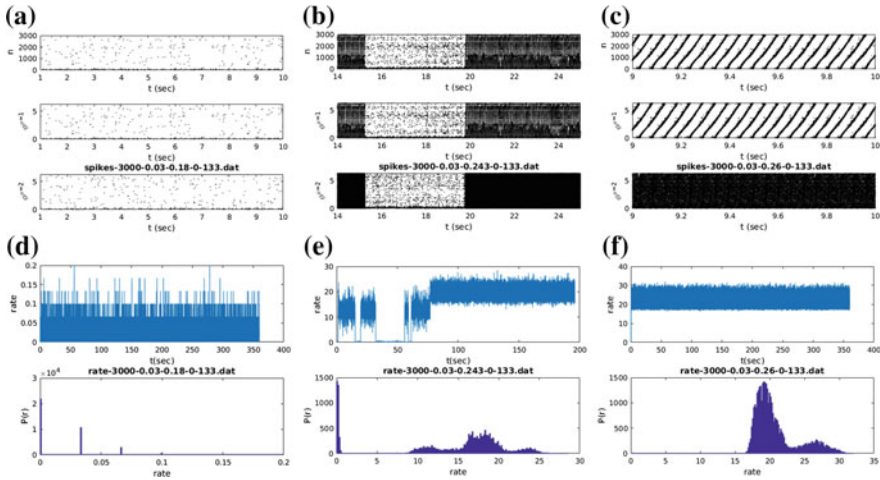


Fig. 9.2 Raster plot is the graphic in which we have the index neuron on the y-axis and the firing time on the x-axis. For each point (α, H_0) of the rate diagram we want to investigate, in figure **a**, **b** and **c** we show three raster plot, in the first one (*upper*) the neurons are ordered according to their own number, in the second one (in the *middle*) are ordered according to the pattern 1 and in the third one (*bottom*) according to the pattern 2. **a** The raster plot shows a quiescence regime in which few neurons fire and without a scheme, for $\alpha = 0.03 \text{ ms}^{-1}$ and $H_0 = 0.18$. **b** An intermitted reactivation of pattern 1, for $\alpha = 0.03 \text{ ms}^{-1}$ and $H_0 = 0.243$. This values of α and H_0 don't allow the permanence of pattern. **c** We have the permanence of retrieval pattern 1, for $\alpha = 0.03 \text{ ms}^{-1}$ and $H_0 = 0.26$. In this model the two patterns can't be retrieve at the same time, so that if we observe the perfect pattern 1, when neurons are ordered according to pattern 2 we observe a lot of neurons fire, because of high firing rate, but in disordered way. In figure **d**, **e** and **f** we show the rate to time (*upper*) and the distribution of rate (*bottom*) of the same point of figure **a**, **b** and **c** respectively. **d** The quiescence regime is shown, few neurons fire during the investigated time interval, indeed the distribution of rate has one peak at low value of rate, close to 0. **e** The bimodal activity and the alternation of up and down states are shown. We observe in *upper figure* the alternation of high and low values of firing rate in time. In the *bottom*, the distribution of rate has two peaks, one close to 0 and another one at higher value of rate. **f** An UP state. The rate always is high and the distribution of rate is similar to a Gaussian distribution with the mean value at high value of rate (about 20)

of rate and normalized variance to a regime of high correlated activity, characterized by high value of both rate and normalized variance. Between these two regime there is the transition region (in blue circle) when the transition occurs. Indeed in figure (d) and (e) we have respectively rate and normalized variance in function of H_0 for fixed value of $\alpha = 0.03 \text{ ms}^{-1}$ and in function of α for fixed value of $H_0 = 0.3$. The peak of normalized variance in correspondence of a growth of rate is the sign that a phase transition occurs. While in the region of high activity (red points in Fig. 9.1b) there is a replay of one of stored pattern (Fig. 9.2c, f), in the region with low rate (yellow points in Fig. 9.1b) there is uncorrelated Poissonian activity (see Fig. 9.2a, d). Between this two regions there is an interval of parameters where both the high-rate and low-rate states are metastable and the system switches between the two states (Fig. 9.2b, f). Even if this is not an equilibrium phase transition, but a dynamical one,

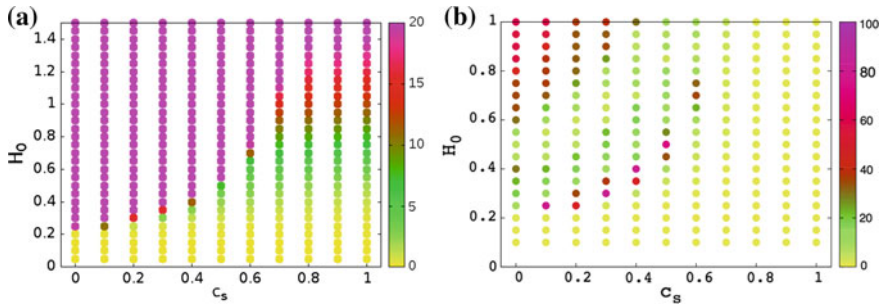


Fig. 9.3 Rate (a) and normalized variance (b) as a function of fraction of shuffled connections c_s , at $\alpha = 0.05 \text{ ms}^{-1}$ and at different values of H_0 . When c_s increases the transition goes to upper values of H_0 , until to a particular value of c_s close to 0.7 where the transition ends. Indeed before this value of c_s , for each c_s we observe the gradually growth of rate and an abrupt increase of normalized variance following by low values again. At upper values of $c_s = 0.7$ the normalized variance is always close to 1 (as we have said) even if the rate increases with H_0

this is similar to a first order transition since effects of hysteresis have been observed by preliminary investigations (not shown).

The raster plot (Fig. 9.2) confirms the idea that a phase transition between a high rate replay regime and a quiescence regime occurs. In raster plots we can see which neuron and when fires. We show three raster plot in order to point out the three different behaviors of the network dynamics: (A) quiescence state, that we call DOWN state, for $\alpha = 0.03 \text{ ms}^{-1}$ and $H_0 = 0.18$, in which few neurons fires, (B) a critical behaviors in which there is an intermitted reactivation of one of stored patterns, for $\alpha = 0.03 \text{ ms}^{-1}$ and $H_0 = 0.243$ (C) high correlated activity for $\alpha = 0.03 \text{ ms}^{-1}$ and $H_0 = 0.26$, in which neurons fire, retrieving perfectly one of stored patterns.

The dynamics of this neural network with structured connectivity is radically altered when its topology changes when we apply the shuffling procedure. It should be emphasized that the strength of connections are the same, even if we shuffle them.

In Fig. 9.3 the rate and normalized variance are shown as function of strength of connection H_0 and fraction of shuffled connections c_s , for fixed value of noise level $\alpha = 0.05 \text{ ms}^{-1}$. This two figures explain how the transition between the two different regimes (from quiescence-DOWN state to correlated activity-UP state) moves to higher values of H_0 as long as c_s increases, until it disappears for a particular value of c_s close to 0.7. Indeed for c_s larger than this particular c_s the normalized variance always is close to 1, index of dynamics dominated by Poissonian noise, so the transition is ended.

In particular we analyze two cases, different from the previous one of structured connectivity ($c_s = 0$): the case near the end of phase transition, choosing $c_s = 0.63$ (63% of connections are shuffled) and the case in which the network has a random connectivity ($c_s = 1$, i.e. all the connections are shuffled).

In Fig. 9.4 we underline the end of phase transition when we shuffle all the connections. The sign of the end of this transition is the disappearing of peak in normalized variance and the gradual growth (very smooth) of firing rate when H_0 increases.

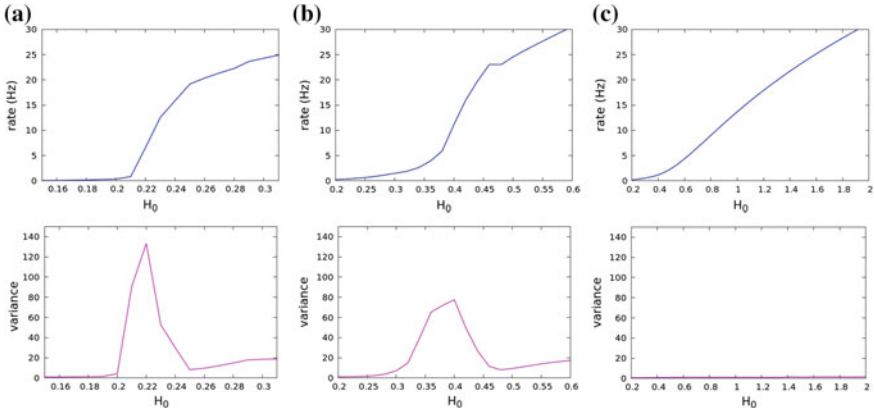


Fig. 9.4 Phase transition ends when we shuffle all the connections, keeping unchanged their values. Three cases are analyzed: **a** $cs = 0$, structured connectivity. The rate increases abruptly and the normalized variance has a peak in correspondence of this increasing of rate. **b** $cs = 0.63$, 63% of connections are shuffled. The increasing of rate is less abrupt than the figure **a** and the normalized variance has a smaller peak moved to higher values of H_0 , like as the transitions moves to higher values of strength of connections but doesn't disappear. **c** $cs = 1$, all the connections are shuffled, but their values don't change. The firing rate increases very smoothly with the increasing of strength of connections, while the peak of normalized variance (seen in previous figures) disappears. The normalized always is close to 1, index of absence of the transition

The intermediate case, $cs = 0.63$ is very interesting. The phase transition occurs at high value of H_0 and at low noise, while at high noise there is a region of high rate but uncorrelated activity (normalized variance is close to 1). In particular at fixed value of $H_0 = 0.8$ (Fig. 9.5), for high value of noise ($\alpha = 0.2 \text{ ms}^{-1}$) we have high value of rate but low value of normalized variance, close to 1, like in the case $cs = 1$ (see later). Indeed the raster plot shows a dynamics in which neurons fire a lot, but without a particular order (see Fig. 9.5b, d). For low value of noise ($\alpha = 0.02 \text{ ms}^{-1}$), the situation is similar to the case of $cs = 0$, because in this case we observe a transition region with a peak of normalized variance. Indeed for this point the raster plot shows a perfect retrieval pattern (see Fig. 9.5a, c). The phase transition moves toward higher values of H_0 and lower values of noise level, when we increase the fraction cs of shuffled connections.

We repeat the same investigation for $cs = 1$. $cs = 1$ means that we shuffle all the connection, getting a completely random connectivity (while the set of connection's strengths are preserved). In this case the figures of firing rate and normalized variance are completely different from the case of $cs = 0$ (structured connectivity) and $cs = 0.63$ (intermediate case). While the rate shows a gradually growth (coming from high values of level noise and strength of connections), the normalized variance is always close to 1, even when the rate is high. It is the sign of a dynamics dominated by Poissonian noise. Indeed the raster plot doesn't show a particular scheme, even if the rate is always high (see Fig. 9.6c).

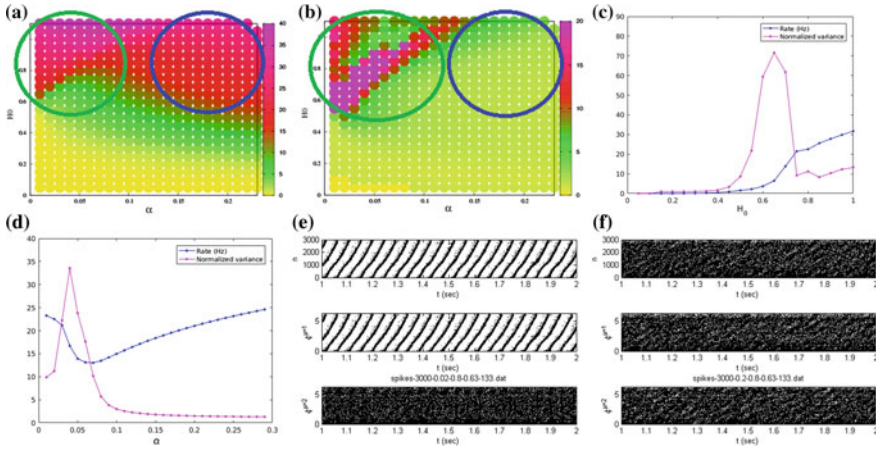


Fig. 9.5 The study of spontaneous dynamics for a network with $cs = 0.63$ (only a fraction of 63% of connections are shuffled). **a** The firing rate shows a gradually growth when we increase the strength of connections, but for high value of noise (in the *blue circle*) the normalized variance **b** is close to 1, similar to the case of $cs = 1$, while for low values of noise (in the *green circle*) the normalized variance shows a peak, similar to the case of $cs = 0$ where we observe a phase transition. **b** Normalized variance diagram, for the same values of α and H_0 of the firing rate diagram. **c** Rate and normalized variance in function of H_0 for fixed value of $\alpha = 0.02 \text{ ms}^{-1}$. We observe a peak of normalized variance when the rate abruptly increases. **d** Rate and normalized variance in function of α for fixed value of $H_0 = 0.8$. We note a peak of normalized variance at value of noise close to 0.04 ms^{-1} , while for high value of α the normalized variance is always close to 1 even if the rate is high. **e** Raster plot of a network with $cs = 0.63$ and $\alpha = 0.02 \text{ ms}^{-1}$ and $H_0 = 0.8$ (*point in the blue circle* of panel **a** and **b**). In this case we observe the perfect retrieval stored pattern with high firing rate. **f** Raster plot of a network with $cs = 0.63$ and $\alpha = 0.2 \text{ ms}^{-1}$ and $H_0 = 0.8$ (*point in green circle* of panel **a** and **b**). Even if the firing rate is high, the neurons fire a lot, but without a precise scheme

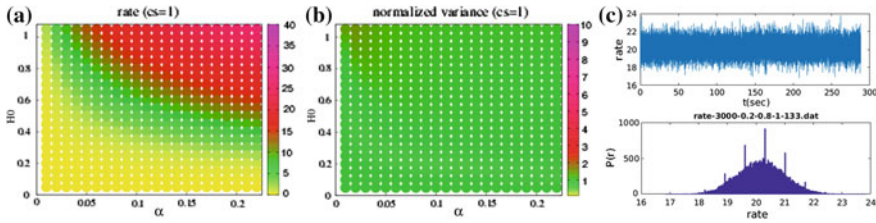


Fig. 9.6 The investigation of firing rate and normalized variance for $cs = 1$ (random connectivity) changing noise level α and strength of connections H_0 gradually. **a** Rate in function of α and H_0 . We note a gradually growth of value of rate for high values of α and H_0 , but this doesn't mean a transition occurs. Indeed in figure **b** we observe values of normalized variance always close to 1, index of dynamics dominated by Poissonian noise. **c** Rate to time (*upper*) and rate distribution (*bottom*) for a network with random connectivity ($cs = 1$), with strength of connection $H_0 = 0.8$ and noise level $\alpha = 0.2 \text{ ms}^{-1}$, i.e. a *red point* in panel **a**. The rate is always high during the investigated time interval and the rate distribution is similar to a Gaussian distribution with a peak at rate close to 20. In the raster plot we don't observe a particular scheme according to which neurons fire

9.4 Conclusion

With this work we have seen how, in a structured network with a phase transition from quiescence state to a replay state, the spontaneous dynamics changes when we shuffle the connections. The balance between excitation and inhibition are preserved during shuffling. The clustering coefficient decreases when the fraction of shuffled connections increases. The clustering coefficient reaches the value that we observe for a completely randomized network when the shuffling fraction is about $cs = 0.7$. This is also the value of cs at which the phase transition seems to disappear. We can conclude that the transition and the rich dynamics in phase-space we observe when the network has a structured connectivity is crucially related to the network topology, induced by the learning procedure. The peak in the normalized variance that we observe near the transition is the signature of a system with high fluctuations as it is observed near a second order transition or near the spinodals of a first order transition. Further investigations are in progress to understand the order of the phase transition.

References

1. Plenzer, D., Kitai, S.: Up and down states in striatal medium spiny neurons simultaneously recorded with spontaneous activity in fast-spiking interneurons studied in cortex-striatum-substantia nigra organotypic cultures. *J Neurosci.* **18**(1), 266–83 (1998)
2. Cossart, R., Aronov, D., Yuste, R.: Attractor dynamics of network UP states in the neocortex. *Nature* **423**, 283–288 (2003). doi:[10.1038/nature01614](https://doi.org/10.1038/nature01614)
3. Shu, Y., Hasenstaub, A., McCormick, D.A.: Turning on and off recurrent balanced cortical activity. *Nature* **423**, 288–293 (2003). doi:[10.1038/nature01616](https://doi.org/10.1038/nature01616)
4. Petersen, C., Hahn, T., Mehta, M., Grinvald, A., Sakmann, B.: Interaction of sensory responses with spontaneous depolarization in layer 2/3 barrel cortex. *PNAS* **100**, 13638–13643 (2003). doi:[10.1073/pnas.2235811100](https://doi.org/10.1073/pnas.2235811100)
5. Luczak, A., Barth, P., Marguet, S.L., Buzski, G., Harris, K.D.: Sequential structure of neocortical spontaneous activity in vivo. *PNAS* **104**, 347–352 (2007). doi:[10.1073/pnas.0605643104](https://doi.org/10.1073/pnas.0605643104)
6. Kinouchi, O., Copelli, M.: Optimal dynamical range of excitable networks at criticality. *Nat. Phys.* **2**, 348–352 (2006). doi:[10.1038/nphys289](https://doi.org/10.1038/nphys289)
7. Deco, G., Jirsa, V.K., McIntosh, A.R.: Resting brains never rest: computational insights into potential cognitive architectures. *Trends Neurosci.* **36**, 268–274 (2013). doi:[10.1016/j.tins.2013.03.001](https://doi.org/10.1016/j.tins.2013.03.001)
8. Shew, W.L., Plenzer, D.: The functional benefits of criticality in the cortex. *Neuroscientist* **19**, 88–100 (2013). doi:[10.1177/1073858412445487](https://doi.org/10.1177/1073858412445487)
9. Scarpetta, S., de Candia, A.: Neural avalanches at the critical point between replay and non-replay of spatiotemporal patterns. *PLoS One* (2013). doi:[10.1371/journal.pone.0064162](https://doi.org/10.1371/journal.pone.0064162)
10. MacLean, J.N., Watson, B.O., Aaron, G.B., Yuste, R.: Internal dynamics determine the cortical response to thalamic stimulation. *Neuron* **48**, 811–823 (2005). doi:[10.1016/j.neuron.2005.09.035](https://doi.org/10.1016/j.neuron.2005.09.035)
11. Lau P-M., Bi G-Q.: Synaptic mechanisms of persistent reverberatory activity in neuronal networks. *Proc. Nat. Acad. Sci. USA* **102**, 10333–10338 (2005). doi:[10.1073/pnas.0500717102](https://doi.org/10.1073/pnas.0500717102)
12. Ji, D., Wilson, M.A.: Coordinated memory replay in the visual cortex and hippocampus during sleep. *Nat. Neurosci.* **10**, 100–107. doi:[10.1038/nn1825](https://doi.org/10.1038/nn1825) (2007)

13. Feng, H., Caporale, N., Yang, D.: Reverberation of recent visual experience in spontaneous cortical waves. *Neuron* **60**, 321–327 (2008). doi:[10.1016/j.neuron.2008.08.026](https://doi.org/10.1016/j.neuron.2008.08.026)
14. Luczak, A., MacLean, J.: Default activity patterns at the neocortical microcircuit level. *Front Integr. Neurosci.* **6**, 30 (2012). doi:[10.3389/fnint.2012.00030](https://doi.org/10.3389/fnint.2012.00030)
15. Ribeiro, T.L., Ribeiro, S., Copelli, M.: Repertoires of spike avalanches are modulated by behavior and novelty. *Front. Neural Circuits* (2016). doi:[10.3389/fncir.2016.00016](https://doi.org/10.3389/fncir.2016.00016)
16. Gerstner, W., Kistler, W.: *Spiking Neuron Models: Single Neurons, Populations, Plasticity*. Cambridge University Press, Cambridge (2002)
17. Watts, S.: Collective dynamics of ‘small-world’ networks. *Nature* **393**, 440–442 (1998). doi:[10.1038/30918](https://doi.org/10.1038/30918)